Atmos. Chem. Phys. Discuss., 4, 1665–1689, 2004
www.atmos-chem-phys.org/acpd/4/1665/
SRef-ID: 1680-7375/acpd/2004-4-1665

Atmospheric Chemistry and Physics Discussions

Highly resolved global distribution of tropospheric NO_2 using GOME narrow swath mode data

S. Beirle[1], U. Platt[1], M. Wenig[2], and T. Wagner[1]

[1]Institut für Umweltphysik, Universität Heidelberg, Germany
[2]NASA Goddard Space Flight Center, Greenbelt, MD 20771, USA

Received: 20 January 2004 – Accepted: 16 February 2004 – Published: 16 March 2004

Correspondence to: S. Beirle (beirle@iup.uni-heidelberg.de)

Abstract

The Global Ozone Monitoring Experiment (GOME, since 1995) allows the retrieval of global total column densities of atmospheric trace gases, including NO_2. Tropospheric vertical column densities (VCDs) are derived by estimating the stratospheric fraction from measurements over the remote ocean. Mean maps of tropospheric NO_2 VCDs derived from GOME clearly allow to detect regions with enhanced industrial activity, but the standard spatial resolution of the GOME ground pixels ($320\times40\,km^2$) is insufficient to resolve regional trace gas distributions or individual cities.

Within the nominal GOME operation, every tenth day measurements in the so called narrow swath mode are executed with a much better spatial resolution ($80\times40\,km^2$). Though the global coverage of these data is – due to the narrow swath – rather poor, the mean distribution over several years (1997–2001) allows to construct a much more detailed picture of the global NO_2 distribution, especially if corrected for seasonal effects. It vividly illustrates the shortcomings of the standard size GOME pixels and reveals an unprecedented wealth of details in the global distribution of tropospheric NO_2. Sharply localised spots of enhanced NO_2 VCD can be associated directly to cities, large power plants, and heavy industry centers.

The long time series of GOME data allows a quantitative comparison of the narrow swath mode data to the nominal resolution that holds general information on the dependency of NO_2 VCDs on pixel size. This is important for new instruments like SCIAMACHY (launched March 2002 on ENVISAT) or OMI and GOME II (to be launched 2004 and 2005, respectively) with an improved spatial resolution.

1. Introduction

The atmospheric composition has changed dramatically over the last 150 years due to the industrial revolution. Among the various emitted pollutants nitrogen oxides ($NO+NO_2=NO_x$ and reservoirs) play an important role. In the troposphere they have

ACPD

4, 1665–1689, 2004

a large impact on human health, climate and atmospheric chemistry, e.g. through their role in catalytic ozone production and their influence on the OH concentration. Moreover, the estimation of the strengths of the different NO_x sources (industry, biomass burning, aircraft, soil emissions, lightning) still has high uncertainties (e.g. Lee et al., 1997), with anthropogenic NO_x (fossil fuel combustion) estimated to account for more than 50% of the overall production. Anthropogenic sources are distributed quite inhomogeneously around the globe and are concentrated in highly populated and industrialized areas, where NO_x is produced by traffic, power generation, heavy industry and domestic combustion.

Satellite measurements are a powerful tool for monitoring trace gas emissions, since the whole globe is observed with a single instrument over long periods of time. The general features of the global distribution of tropospheric NO_2 have been reported in several studies (Leue et al., 2001; Velders et al., 2001; Wenig, 2001; Richter and Burrows, 2002; Martin et al., 2002) using data from the Global Ozone Monitoring Experiment (GOME) on board the ESA satellite ERS-2, launched in April 1995 (Burrows, 1999). These studies clearly showed, that satellite observations have the potential to identify different sources of tropospheric NO_x, in particular the industrialized areas of the world (e.g. the USA, central Europe, China). However, the standard spatial resolution of one GOME ground pixel ($320\times40\,km^2$) is insufficient to resolve details of the regional NO_2 distribution or individual cities. To improve our knowledge of the distribution of NO_2 burden, i.e. the location and extent of sources and the role of transport, and to potentiate quantitative estimates of emissions, a better spatial resolution is essential.

2. Retrieval

2.1. Tropospheric NO_2 VCD from GOME

The ERS-2 satellite flies along a sun-synchronous polar orbit and crosses the equator at 10:30 a.m. (local time). GOME consists of four spectrometers measuring the radiation reflected by the earth in the UV/vis spectral range (240–790 nm) with a resolution of about 0.2–0.4 nm. Global coverage at the equator is achieved every three days. Column densities of several trace gases can be determined, applying Differential Optical Absorption Spectroscopy (DOAS) (Platt, 1994). The retrieval of vertical column densities (VCDs) of NO_2 is described in detail in Wagner (1999) and Leue et al. (2001).

Since the global distribution of stratospheric NO_2 is much more homogeneous in space and time than in the troposphere, it is possible to estimate the stratospheric fraction of the total column (e.g. Leue et al., 2001; Velders et al., 2001; Wenig, 2001). Systematic errors in the total column due to the degradation of the GOME instrument or the diffuser plate (Richter and Wagner, 2001) are included in the stratospheric estimation, and thus will not affect the resulting tropospheric column. For this study, the latitude dependent stratospheric column of NO_2 was determined in a reference sector over the remote Pacific (Richter and Burrows, 2002). The difference between the total and the stratospheric column represents the tropospheric fraction. For a quantitative analysis these values have to be corrected for the reduced sensitivity of GOME towards tropospheric trace gases. The absolute value of the correction factor depends on trace gas profile, earth albedo, cloud fraction and aerosol load (Leue et al., 2001; Wagner et al., 2001 (BrO); Richter and Burrows, 2002; Martin et al., 2003). In this study, we apply a uniform correction factor of 2, to keep the analysis as elementary as possible and to avoid uncertainties emerging from external data. The actual column is probably higher due to the shielding effect of clouds (Richter and Burrows, 2002; Wagner et al., 2003). However, we do not correct for the cloud fraction, since its influence is not fully understood (see below) and differs regionally (Wenig, 2001).

2.2. GOME spatial resolution and narrow swath mode

GOME scans the Earth's surface by moving the scan mirror by ±31°, corresponding to a cross track swath width of 960 km. During each scan, three ground pixels are mapped with a spatial resolution of 320 km east-west and 40 km north-south, followed by one backscan pixel with an extent of $960 \times 40\,km^2$ (see Fig. 1).

ACPD
4, 1665–1689, 2004

Besides this standard size mode (referred as SSM below), GOME has the possibility to reduce the range of the scan mirror angle. This is done since end of June 1997: an angular range of ±8.7° is applied three days a month, namely the 4th/5th, the 14th/15th and the 24th/25th of every month between the sun calibrations of those days. These measurements in the so called narrow swath mode (referred as NSM below) have a spatial resolution of 80×40 km^2 (forward scan) and 240×40 km^2 (backscan), respectively (see Fig. 1). Additional information on the GOME viewing geometry is described in the GOME users manual (Bednarz, 1995).

The NSM improves the spatial resolution, but the global coverage is reduced: in the SSM GOME reaches global coverage each 3 days, while for the NSM 12 measurement days are required. Since the NSM is only applied every 10th day, statistically 120 days are needed to reach a global cover with the NSM orbits. Figure 2 shows the total number of measurements in the NSM during the 5 year period from 1997 to 2001 around the globe.

2.3. High quality map from high resolution NSM data

Figure 3a shows a global map of the mean tropospheric NO_2 VCD, using the SSM (320 km by 40 km) GOME pixels 1996–2001 (no backscans). Regions of industrial activity show significantly enhanced VCDs. Also the influence of biomass burning and high lightning activity is detectable (e.g. Leue et al., 2001; Richter and Burrows, 2002; Beirle et al., 2003). However, the emissions of comparably small sources like single cities are “smeared out” due to the large east-west extension of the GOME ground pixels.

Figure 3b depicts the mean tropospheric NO_2 VCD of all NSM pixels during 1997–2001. The better spatial resolution reveals many more details of the global distribution of tropospheric NO_2. But whereas Fig. 3a shows a quite smooth distribution, Fig. 3b exhibits stripe like patterns parallel to the ERS-2 flight direction.

The reason for these stripes is the sparse global coverage. In the NSM, each point on the Earth is scanned only about 10-15 times during a six year time period (Fig. 2).

Moreover, these measurements are not distributed homogeneously over the year. Especially for regions where the NO_2 burden varies with season (e.g. due to biomass burning), the actual date of the measurement becomes essential. This is illustrated in Fig. 4 for the case of Central Africa, a region with yearly biomass burning events from June to September. Two neighbouring locations are selected, showing (A) a high and (B) a quite low tropospheric NO_2 VCD. In Table 1, the dates of measurements in the NSM are listed for both locations. Whereas all (but one) scans of location A were made during the burning season, only one out of thirteen scans took place in the burning season for location B. So the main reason for the stripe structure is the fact that the local measurements are not distributed uniformly throughout the year. Therefore we call it the "seasonal effect", since the measured NO_2 VCD depends on the season in which the majority of the measurements were made.

Seasonal variations should not be influencing a multi-year average. The stripe structure could be reduced by spatially smoothing the data. However, it is the whole idea of this investigation to obtain a map of the NO_2 distribution with improved resolution from the NSM data. Therefore, to account for the patchy temporal coverage, we apply a more sophisticated correction of the seasonal effect. For this procedure we use our knowledge of the mean distribution of NO_2 VCD from the SSM as seen in Fig. 3a: Each GOME measurement consists of three forward scan pixels and a subsequent backscan pixel (see Fig. 1). The spatial resolution ($240\times40\,km^2$) of the backscan pixel in the NSM is quite comparable to the extent of the SSM forward scan pixels. Hence we can estimate the seasonal offset for each individual NSM measurement by comparing the NSM backscan VCD with the mean of all SSM pixels at the same location, and correct the NSM forward scan pixels by this "offset".

The resulting seasonally corrected mean tropospheric NO_2 VCD distribution of the NSM pixels is shown in Fig. 3c, which is free of the stripelike structures of Fig. 3a. The remaining noisy values around South America are due to the South Atlantic anomaly (Heirtzler, 2002).

ACPD
4, 1665–1689, 2004

Title Page
Abstract | Introduction
Conclusions | References
Tables | Figures
◀◀ | ▶▶
◀ | ▶
Back | Close
Full Screen / Esc
Print Version
Interactive Discussion

3. Global distribution of tropospheric NO_2

Figure 3c reveals many details on the tropospheric NO_2 distribution. In the polluted areas in North America, Europe, the Middle East and Far East, structures can be seen with unprecedented spatial resolution. Many "hot spots" show up, and sources of NO_2 can be clearly localized and identified (mostly large cities). Even the highly populated Nile river valley in Egypt is visible. On the other hand, tropical regions of enhanced NO_2 VCD like Congo show no new spatial information, since the sources (biomass burning, lightning) are not sharply localized in the mean taken over several years.

To illustrate the new insight in the tropospheric NO_2 distribution from NSM data in detail, Fig. 5 displays zooms of Fig. 3c for (a) North America and (b) Europe as examples. Additionally, the location of larger cities is marked, and in (b) contour lines (1 km altitude) indicate mountains.

In the USA, nearly each major city can be associated directly to a NO_2-"hot spot" in Fig. 5a, and vice versa. Nevertheless, there also is a significant area of elevated NO_2 in a remote region (marked white in Fig. 5a). This is due to a field of large coal power plants (e.g. "Four Corners" with a capacity of 2 GW, see referenced weblinks). The spot in North Mexico (marked grey) is associated with coal power plants as well ("Carbon 1/2", Piedras Negras).

Also in Europe, the NO_2 load generally reflects human activity. Major cities (e.g. Moscow, Madrid, Istanbul or London) show enhanced levels of NO_2, like in the USA. However, there are also some cities with more than 1 million inhabitants (e.g. Rome, Berlin, Warsaw), that show rather low levels of NO_2, while the highest levels of NO_2 are found in some industrial areas (Po Valley, Ruhr area). These data might help to quantify the different anthropogenic sources (traffic via industry) separately.

ACPD

4, 1665–1689, 2004

4. Extent of NO_2 pollution "hot spots"

Though the number of available NSM observations for each given location is rather small (see Fig. 2), the "hot spots" detected round the globe are rich in contrast and have well defined edges. Apart from congested areas like the US Eastcoast, western Europe or east China, where large regions show enhanced NO_2 levels, there are several NO_2 peaks according to large cities that are comparable in their spatial extent (see Fig. 3c). The Istanbul plume, as a typical example, ranges approx. 80 km in east-west (i.e. the width of the NSM!) and 50 km in north-south-direction (the higher east-west-extent is likely to reflect the GOME ground pixel geometry). Less than 80km aside from the plume center the NO_2 VCD is already on the normal background level. Therefore, only the tracks directly crossing the source see an enhanced NO_2 VCD.

4.1. Lifetime of boundary layer NO_x

The low spatial extent of the hot spots and the sharp decrease of NO_2 VCD at their edges indicate that the average lifetime of NO_x in the lower troposphere must be rather small. To give a rough quantitative estimation, we assume a first order, i.e. exponential loss of NO_x with a constant lifetime τ throughout the year. In a distance of approx. 60 km the VCD is dropped to 1/e. The distance is related to the time via $x=v\tau$, with v being the mean wind speed. For v=1 m/s (as a lower limit) this results in a mean lifetime of about τ=60 km/1 (m/s) ≈17 h, and less for higher mean wind speeds. Although this is a very rough estimation, the mean lifetime of NO_2 in the boundary layer obviously can not be much larger than a day, since otherwise an offwind plume should be detectable in the NSM data. So NSM GOME observations allow to derive an upper limit to the lifetime of boundary layer NO_2, and thus NO_x, for sites around the globe. (Beirle et al., 2003, used GOME data to estimate the NO_x lifetime of 6 h in summer and 24–36 h in winter for Germany).

ACPD
4, 1665–1689, 2004

4.2. NSM via SSM resolution

In the SSM, pollution peaks are obviously "smeared out" due to the 320 km width of the GOME pixel in west-east-direction (see Fig. 3a; compare, for instance, the shape of the Hong Kong peak in 3a and 3c). For the same reason the maximal VCDs measured in the SSM are lower than in the NSM. A quantitative estimation of this effect is illustrated in Fig. 6: A given (Gaussian) distribution of NO_2 pollution with a FWHM of 20, 50, 100 or 200 km (i.e. the extent of large cities or congested areas) is scanned with pixels of NSM and SSM size respectively. The actual VCD is drastically underestimated by SSM observations at its peak, but overestimated at its edges. This effect is much weaker for the NSM, since its resolution approaches the actual extent of the NO_2 distribution. Figure 6 also displays the ratio of the modelled maxima in the NSM and the SSM, which was found to be close to 4 for a point source and approaches unity for extended sources. Table 2 now lists the actual measured NO_2 VCDs over some selected cities for the NSM and the SSM. As expected, the NSM observations show higher VCDs. A comparison of the measured NSM/SSM ratios in Table 2 with those calculated in Fig. 6 also allows to deduce the spatial extent of the sources. Mexico city, for instance, where the NSM/SSM-ratio is 3.2, can be regarded as an isolated source spot with an extent of <80 km. The Ruhr Area, on the other hand, where the NSM/SSM ratio is only 1.46, has a large extent and is probably also affected by sources in the Netherlands and Belgium.

To further analyse the "smoothing effect" for SSM measurements, we plotted the difference of the NSM forwardscans (i.e. high resolution observations), and the NSM backscans (representing nearly the SSM resolution), in Fig. 7 (for the same clippings as in Fig. 5). The dipolar structure indicated in Fig. 6 (i.e. the underestimation of the SSM observations above the spot and underestimation left and right) is impressively illustrated in Fig. 7, especially for isolated cities (Mexico City, Madrid, Salt Lake City, Phoenix) and cities with very high NO_2 VCDs (Los Angeles). This plot indicates the location and the extent of sources even better than Fig. 5, especially for "hot spots"

ACPD

4, 1665–1689, 2004

Highly resolved global distribution of tropospheric NO_2

S. Beirle et al.

in polluted regions. The Po valley, for instance, is generally highly polluted by Milan emissions. Figure 7, however, reveals that there are at least two more hot spots, namely Turin and Padua/Venice.

Furthermore, Fig. 7 clearly displays locations where the SSM GOME observations overestimate the actual burden due to the ”smearing out” of local peaks. This is a valuable additional information for the interpretation of GOME studies. For instance, the mean of the SSM GOME pixels (Fig. 3a) shows enhanced VCD of NO_2 over the North Sea between England and the Netherlands. Figure 7 shows that these VCDs are overestimated. So, the observed enhancement is not only due to transport by wind as may be assumed, but also to the fact that each nominal pixel in this area either covers polluted sites in England (Manchester, Sheffield etc.) or the Netherlands (Rotterdam). The VCD over the western Alpine mountains is also drastically overestimated by the SSM observations due to the short distance to Milan.

5. Influence of the cloud fraction on the mean VCD

Boundary layer NO_2 may be shielded by clouds. Due to the high cloud albedo, this effect is nonlinear: the average of two half clouded pixel results in a VCD different from the mean of one cloud free and one totally clouded pixel (e.g. Wenig, 2001; Richter and Burrows, 2002; see also Fig. 8).

Since the NSM is sampled with a 4 times higher spatial resolution, those pixels are more often cloud free than SSM pixels: For the US, for instance, the percentage of cloud free (i.e. having cloud fraction below 10%) pixels is 34.7% in the SSM and 40.7% in the NSM (Cloud fraction taken from the HICRU database, Grzegorski, 2003).Therefore (and for the aforementioned reason) we would expect the NSM forwardscan observations to yield generally higher VCDs than SSM or NSM backscans respectively.

To analyse this effect, in Fig. 9 we compared the NSM backscan with the weighted average of the respective forwardscans that it covers.

Surprisingly, we find a linear relation with a slope of 0.98, i.e. almost unity. That

ACPD
4, 1665–1689, 2004

means that in contrast to our expectation the pixel size has almost **no** influence on the **mean** NO_2 VCD. Partly, this could be explained by a significant amount of NO_2 above the clouds (Wenig, 2001; Richter and Burrows, 2002). On the other hand, it is obvious, that in many polluted regions the tropospheric NO_x is close to the ground. At present, we do not understand our findings and intend to present a detailed analysis of the dependency of cloud fraction distributions on pixel size and the relating radiative transfer aspects in a future study. However, our finding has a high relevance on the quantitative interpretation of the results of GOME and its successors like SCIAMACHY, OMI or GOME II.

6. Conclusion and outlook

The analysis of the GOME observations in the narrow swath mode results in a global map of tropospheric NO_2 with an unmatched spatial resolution ($80\times40\,km^2$). The comparison of forward- and backscans allows to correct for data fluctuations due to the patchy temporal sampling.

The resulting maps (Figs. 3c, 5 and 6) display many "hot spots" which are not visible in the standard GOME observations. Most hot spots can directly be associated with cities. But, even large power plants like "Four Corners" in the USA can be detected. This demonstrates that satellite instruments are capable of detecting and monitoring local pollution and provide valuable additional information on the global distribution of NO_x sources which might be used for comparison and improvement of emission data bases. The quite sharply localised hot spots also indicate a low lifetime of boundary layer NO_x of less than one day, even for cities like Moscow at 56° N.

The problem of poor temporal coverage of the GOME measurements in the narrow swath mode will be resolved by SCIAMACHY (currently in its validation phase) with an even better spatial resolution ($60\times30\,km^2$) and further satellite missions (OMI, GOME II).

The quantitative comparison of NSM forward- and backscan (approximate equivalent

ACPD
4, 1665–1689, 2004

in size to the SSM) observations reveals that the pixel size has nearly no effect on the **mean** NO_2 VCD. This is quite surprising, since the pixel size definitely affects the distribution of fractional cloud fraction. This finding has important consequences on the quantitative interpretation of SCIAMACHY and OMI data (and possible comparisons to GOME).

Acknowledgements. This study was funded by the German Ministry for Education and Research as part of the NOXTRAM project (Atmospheric Research 2000). We like to thank the European Space Agency (ESA) operation center in Frascati (Italy) and the "Deutsches Zentrum für Luft- und Raumfahrt" DLR (Germany) for providing the ERS-2 satellite data. Cloud data was taken from the HICRU data base provided by M. Grzegorski.

Edited by: A. Richter

References

Bednarz, F.: Global Ozone Monitoring Experiment (GOME) Users Manual, Eur. Space Agency Publ. Div., Noordwijk, The Netherlands, 1995.

Beirle, S., Platt, U., Wenig, M., and Wagner, T.: Weekly cycle of NO_2 by GOME measurements: a signature of anthropogenic sources, Atmos. Chem. Phys. 3, 2225–2232, 2003.

Beirle, S., Platt, U., Wenig, M., and Wagner, T.: NO_x production by lightning estimated with GOME, Adv. Space Res., accepted, 2003.

Burrows, J., Weber, M., Buchwitz, M., Rozanov, V., Ladstetter-Weienmayer, A., Richter, A., De Beek, R., Hoogen, R., Bramstedt, K., Eichmann, K. U. , Eisinger, M., and Perner, D.: The Global Ozone Monitoring Experiment (GOME): Mission concept and first scientific results, J. Atmos. Sci., 56, 151–175, 1999.

Four Corners Power Plant: http://www.srpnet.com/power/stations/fourcorners.asp; http://www.pnm.com/systems/4c.htm.

Grzegorski, M.: Determination of cloud parameters for the Global Ozone Monitoring Experiment with broad band spectrometers and from absorption bands of oxygen dimer, Diploma thesis, University of Heidelberg, Germany, 2003.

ACPD

4, 1665–1689, 2004

Highly resolved global distribution of tropospheric NO_2

S. Beirle et al.

Heirtzler, J.: The future of the South Atlantic anomaly and implications for radiation damage in space, J. Atmos. Solar-Terr. Phys., 64, 1701–1708, 2002.
Lee, D. S., Köhler, I., Grobler, E., Rohrer, F., Sausen, R., Gallardo-Klenner, L., Olivier, J. G. J., Dentener, F. J., and Bouwman, A. F.: Estimations of global NO_x emissions and their uncertainties, Atmos. Environ., 31, 1735–1749, 1997.
Leue, C., Wenig, M., Wagner, T., Klimm, O., Platt, U., and Jähne, B.: Quantitative analysis of NO_2 emissions from GOME satellite image sequences, J. Geophys. Res., 106, 5493–5505, 2001.
Martin, R. V., Chance, K., Jacob, D. J., Kurosu, T. P., Spurr, R. J. D., Bucsela, E., Gleason, J. F., Palmer, P. I., Bey, I., Fiore, A. M., Li, Q., Yantosca, R. M., and Koelemeijer, R. B. A.: An improved retrieval of tropospheric nitrogen dioxide from GOME, J. Geophys. Res., 107, D20, 4437, doi:10.1029/2001JD001027, 2002.
Martin, R. V., Jacob, D. J., Chance, K., Kurosu, T. P., Palmer, P. I., Evans, M. J.: Global inventory of nitrogen oxide emissions constrained by space-based observations of NO_2 columns, J. Geophys. Res., 108, 4537, doi:10.1029/2003JD003453, 2003.
Platt, U.: Differential optical absorption spectroscopy (DOAS), in Air Monitoring by Spectrometric Techniques, edited by Sigrist, M., Chemical Analysis Series, 127, 27–84, John Wilsy, New York, 1994.
Richter, A. and Wagner, T.: Diffuser Plate Spectral Structures and their Influence on GOME Slant Columns, Technical Note, http://giger.iup.uni-heidelberg.de/thomas/diffuser_gome.pdf, January 2001.
Richter A. and Burrows, J.: Retrieval of Tropospheric NO_2 from GOME Measurements, Adv. Space Res., 29, 11, 1673–1683, 2002.
Velders, G.J.M., Granier, C., Portmann, R.W., Pfeilsticker, K., Wenig, M., Wagner, T., Platt, U., Richter, A., and Burrows, J.: Global tropospheric NO_2 column distributions: Comparing 3-D model calculations with GOME measurements, J. Geophys. Res., 106, 12 643–12 660, 2001.
Wagner, T.: Satellite observations of atmospheric halogen oxides, Ph.D. thesis, University of Heidelberg, Germany, 1999.
Wagner, T., Leue, C., Wenig, M., Pfeilsticker, K., and Platt, U.: Spatial and temporal distribution of enhanced boundary layer BrO concentrations measured by the GOME instrument aboard ERS-2, J. Geophys. Res., 106, 24 225–24 236, 2001a.
Wagner, T., Richter, A., Friedeburg, C. v., Wenig, M., and Platt, U.: Case Studies for the In-

ACPD
4, 1665–1689, 2004

vestigation of Cloud Sensitive Parameters as Measured by GOME, TROPOSAT final report, Sounding the Troposphere from Space: a New Era for Atmospheric Chemistry, Springer, Berlin, 199–210, 2003.
Wenig, M.: Satellite Measurements of Long-Term Global Tropospheric Trace Gas Distributions and Source Strengths, Ph.D. thesis, University of Heidelberg, Germany, http://mark-wenig.de/diss_mwenig.pdf, 2001.

ACPD
4, 1665–1689, 2004

Table 1. Dates of measurements for the sites marked in Fig. 4. Bold typing indicates the **burning season** in Central Africa (June–September).

Site A	Site B
05.09.1997	15.03.1998
25.09.1998	05.05.1998
05.07.1999	05.01.1999
25.08.1999	25.02.1999
25.10.1999	25.05.1999
25.08.2000	**15.07.1999**
25.07.2001	05.12.1999
	25.01.2000
	25.05.2000
	15.10.2000
	05.12.2000
	05.04.2001
	25.12.2001

ACPD
4, 1665–1689, 2004

Table 2. Comparison of NSM and SSM mean tropospheric NO_2 VCD (10^{15} molec/cm^2) for different cities/regions. The third column gives the ratio NSM/SSM, that is compared with the simulations in Fig. 7.

City/region	VCD SSM	VCD NSM	Ratio NSM/SSM
Los Angeles	8.70	22.42	2.58
Phoenix	3.72	7.54	2.03
New York	4.98	8.30	1.67
Mexico City	4.88	15.66	3.21
Ruhr Area	3.94	5.74	1.46
Milan	5.68	8.30	1.46
South Africa	6.56	9.22	1.41
Dschidda	3.18	8.44	2.65
Rijad	4.32	9.68	2.24
Hongkong	6.16	12.86	2.09
Shanghai	4.32	7.84	1.81
Beijing	5.70	8.32	1.46
Seoul	5.46	10.24	1.88
Tokio	4.30	8.74	2.03
Istanbul	2.44	5.56	2.28

ACPD
4, 1665–1689, 2004

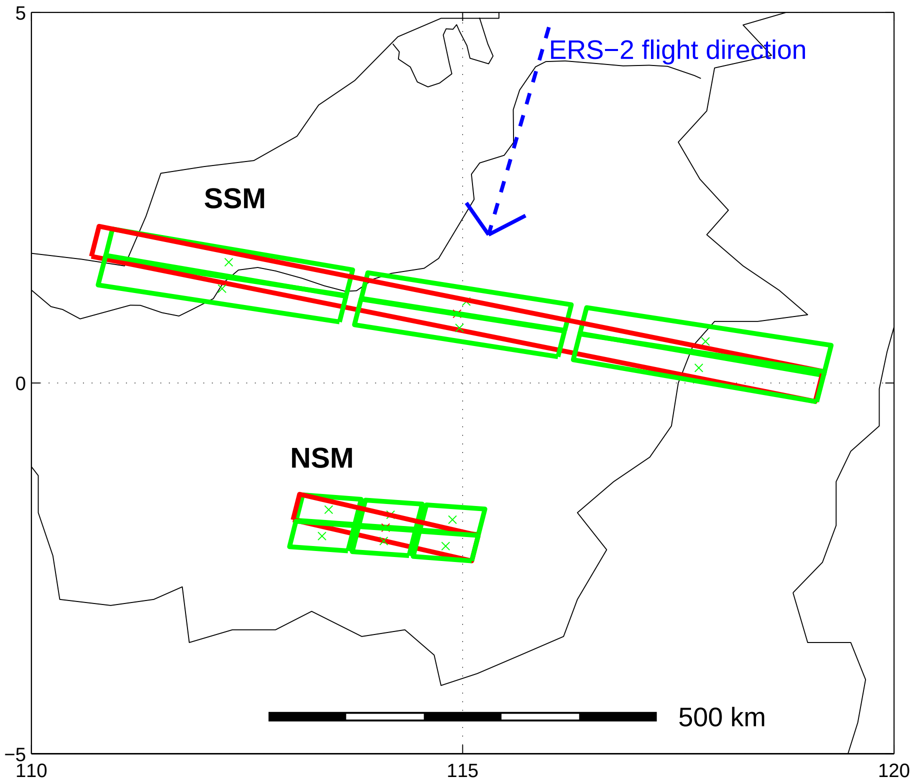

Fig. 1. Spatial extension and geometry of the GOME ground pixels. A snapshot of the standard size mode (SSM, 320×40 km^2) and the narrow swath mode (NSM, 80×40 km^2) is shown at the equator (Borneo). The forward scan pixels are green, the subsequent backscans, having triple length, red.

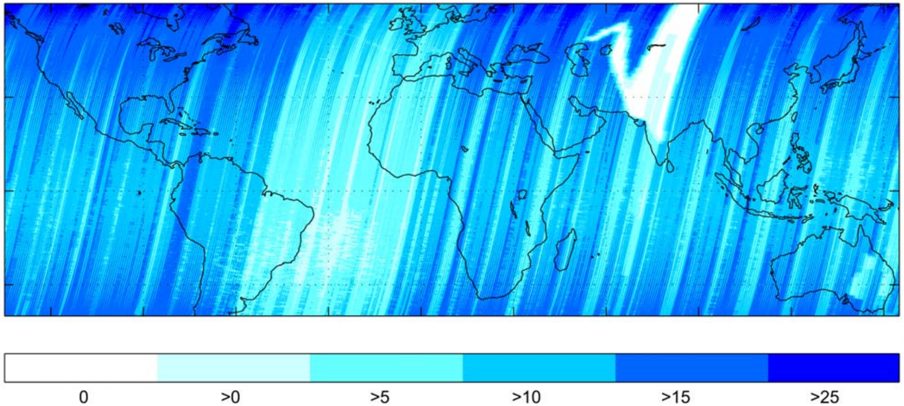

Fig. 2. Total number of GOME scans in the narrow swath mode (NSM) 1997–2001.

ACPD

4, 1665–1689, 2004

Highly resolved global distribution of tropospheric NO_2

S. Beirle et al.

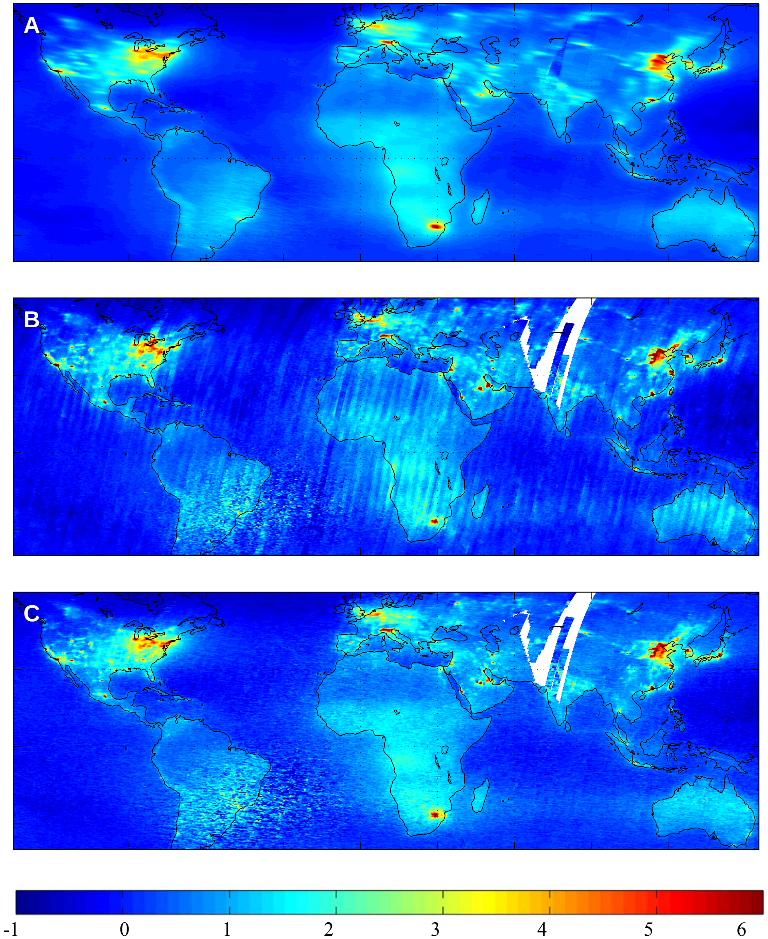

Fig. 3. Global mean of tropospheric NO_2 VCD (10^{15} molecules/cm^2), using **(a)** all nominal pixels 1996–2001 (no backscans), **(b)** NSM pixels only 1997–2001, **(c)** NSM pixels only (1997–2001), corrected for seasonal effects.

ACPD
4, 1665–1689, 2004

Highly resolved global distribution of tropospheric NO_2

S. Beirle et al.

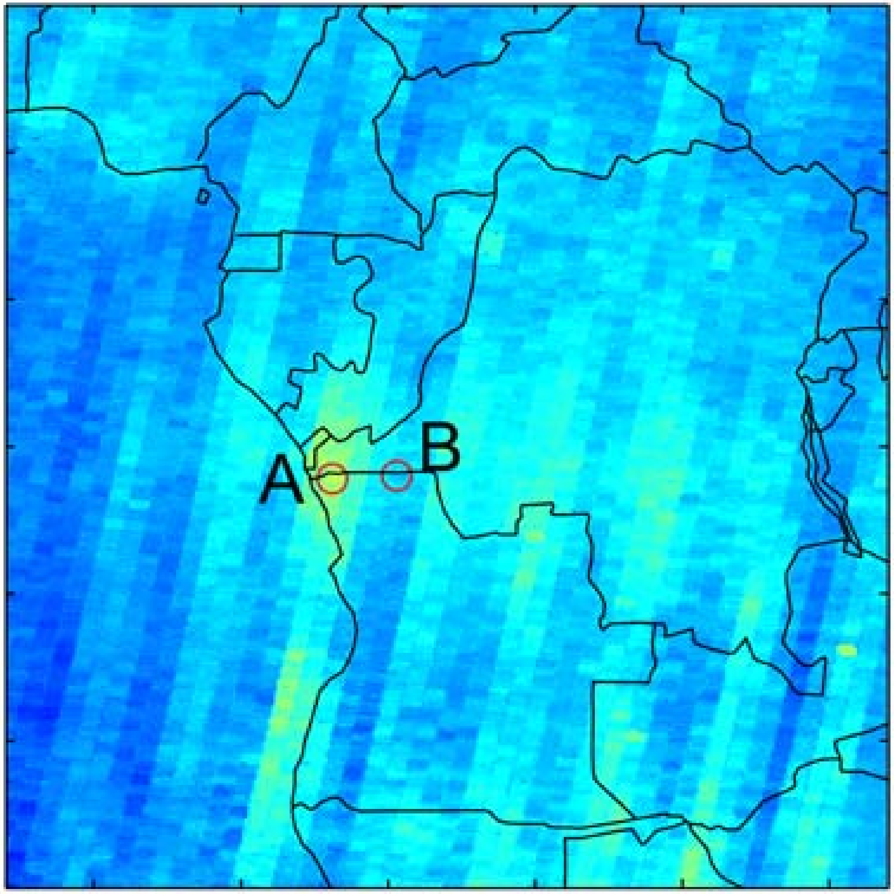

Fig. 4. Zoom of Fig. 3b on Central Africa to explain the stripe like features. Two neighbouring sites with high (A) and low (B) VCD of tropospheric NO_2 are compared. Table 1 reveals that for site (A) almost all (whereas for site (B) only 1) measurements took place during the burning season.

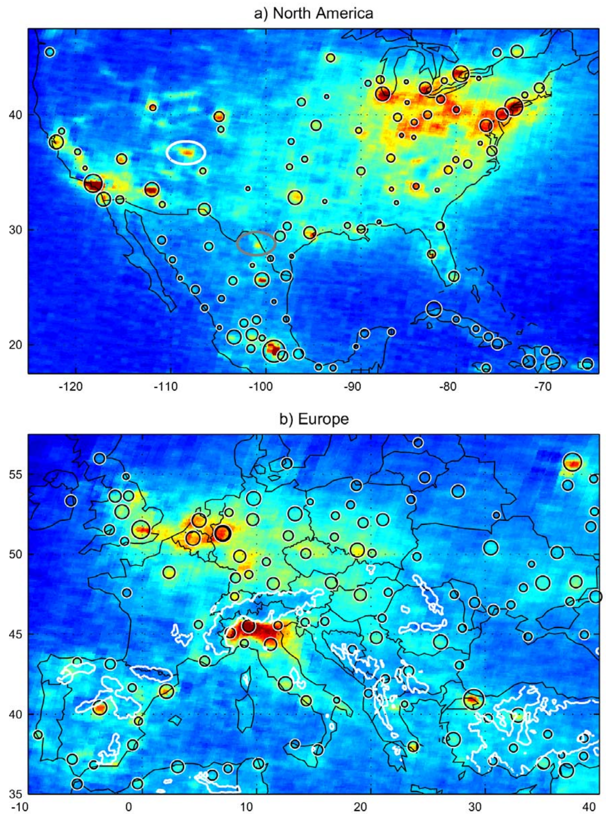

Fig. 5. Zoom of Fig. 3c for North America **(a)** and Europe **(b)**. Cities with more than 200000 (a) and 500 000 (b) inhabitants are marked (cities within a 100 km distance are cumulated). The marked spots in (a) indicate NO_2 pollution that does not coincide with a large city, but instead with large coal fired power plants ("Four Corners", USA (white); "Piedras Negras", Mexico (grey)). For Europe, also the 1 km altitude contour lines are shown illustrating mountains. The projections are equal-area for 35° N (a) and 45° N (b), respectively.

ACPD

4, 1665–1689, 2004

Highly resolved global distribution of tropospheric NO_2

S. Beirle et al.

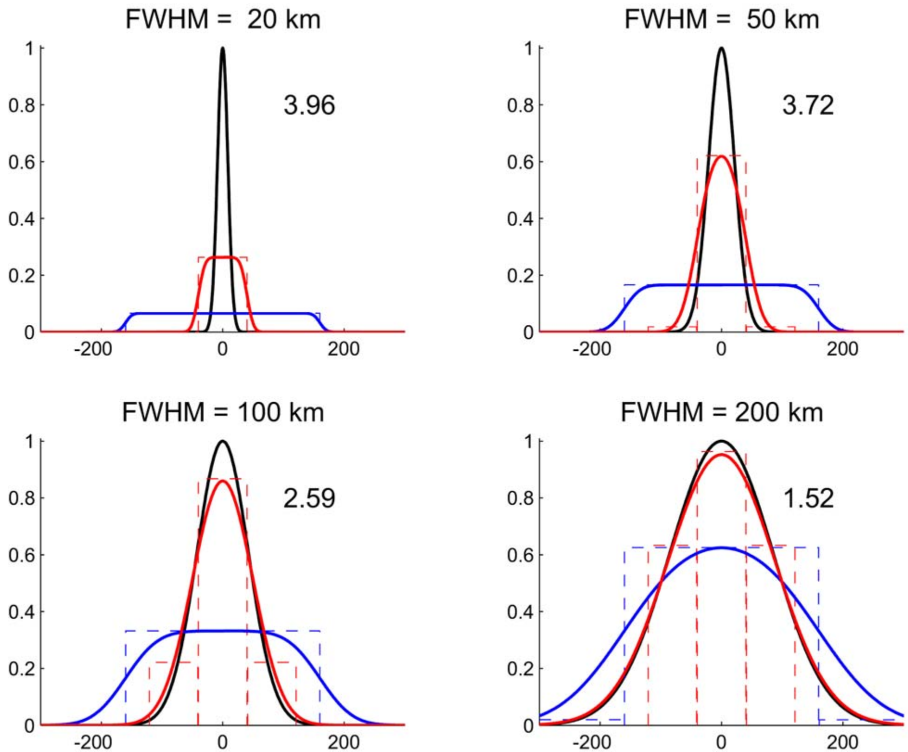

Fig. 6. Illustration of the smoothing effect of the GOME SSM pixels. A given pollution distribution (black), assumed to be Gaussian with different FWHM, is underestimated by GOME SSM (blue) over its maximum, but overestimated over its edges. This effect is much weaker for the NSM (red). The dotted boxes indicate an individual measurement where the middle GOME pixel is centered at the pollution peak; the solid lines display the mean of a large number of measurements at different positions, i.e. the actual pollution distribution convoluted with the GOME resolution. The numbers give the ratio of the measured maximum in the NSM and the SSM.

ACPD

4, 1665–1689, 2004

Highly resolved global distribution of tropospheric NO_2

S. Beirle et al.

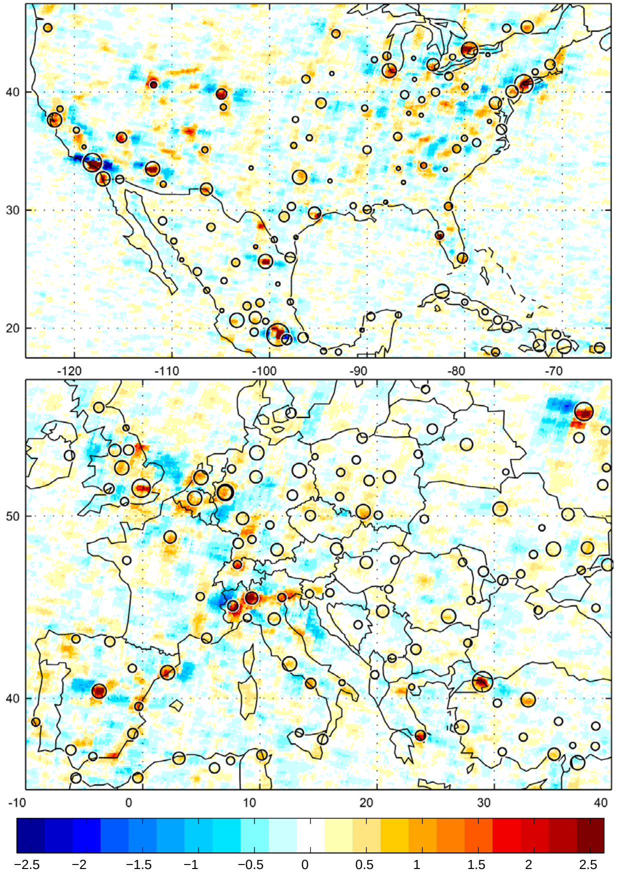

Fig. 7. Difference of the NSM forward- and backscan pixels (10^{15} molec/cm^2) for North America **(a)** and Europe **(b)**. Red spots show locations, where the tropospheric NO_2 column is underestimated by the nominal viewing pixels from GOME (several cities), whereas it is overestimated for the blue spots (e.g. the Alpine mountains).

ACPD

4, 1665–1689, 2004

Highly resolved global distribution of tropospheric NO_2

S. Beirle et al.

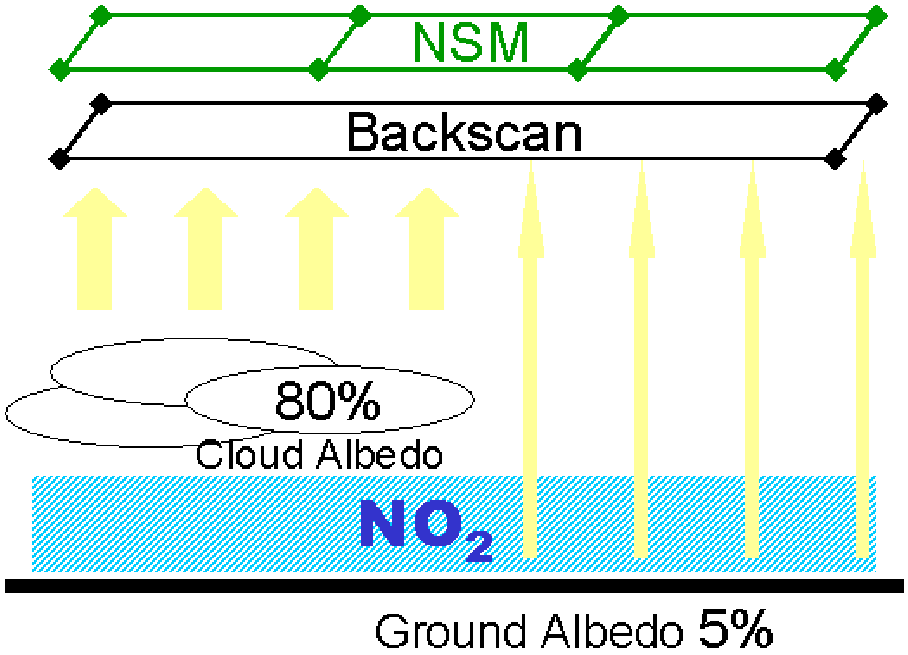

Fig. 8. Shielding effect of clouds For a cloudy scene, boundary layer NO_2 would be shielded and thus be "invisible" for GOME. Furthermore, since the cloud albedo is much higher than the ground albedo, the observed light comes predominantly from the clouds, leading to a further underestimation of boundary layer NO_2. For instance, in the given scene with 50% cloud fraction the reflected light intensity would be $0.5 \times I \times 0.8 + 0.5 \times I \times 0.05 = (0.4 + 0.025) \times I$. I.e. only 6% of the measured light comes from the ground, i.e. has crossed the NO_2 profile. Therefore, in the backscan only 6% of the actual NO_2 column would be detected. In the NSM forward scans there would be one totally cloudy pixel (seeing no NO_2), one pixel with 50% cloud fraction (seeing 6% as for the backscan) and one cloud free pixel (seeing 100% of the actual NO_2 column!). In average, the NSM forward scans would detect $(0+0.06+1)/3=35\%$ of the boundary layer NO_2, i.e. 6 times as much as for the backscan observation!

ACPD

4, 1665–1689, 2004

Highly resolved global distribution of tropospheric NO_2

S. Beirle et al.

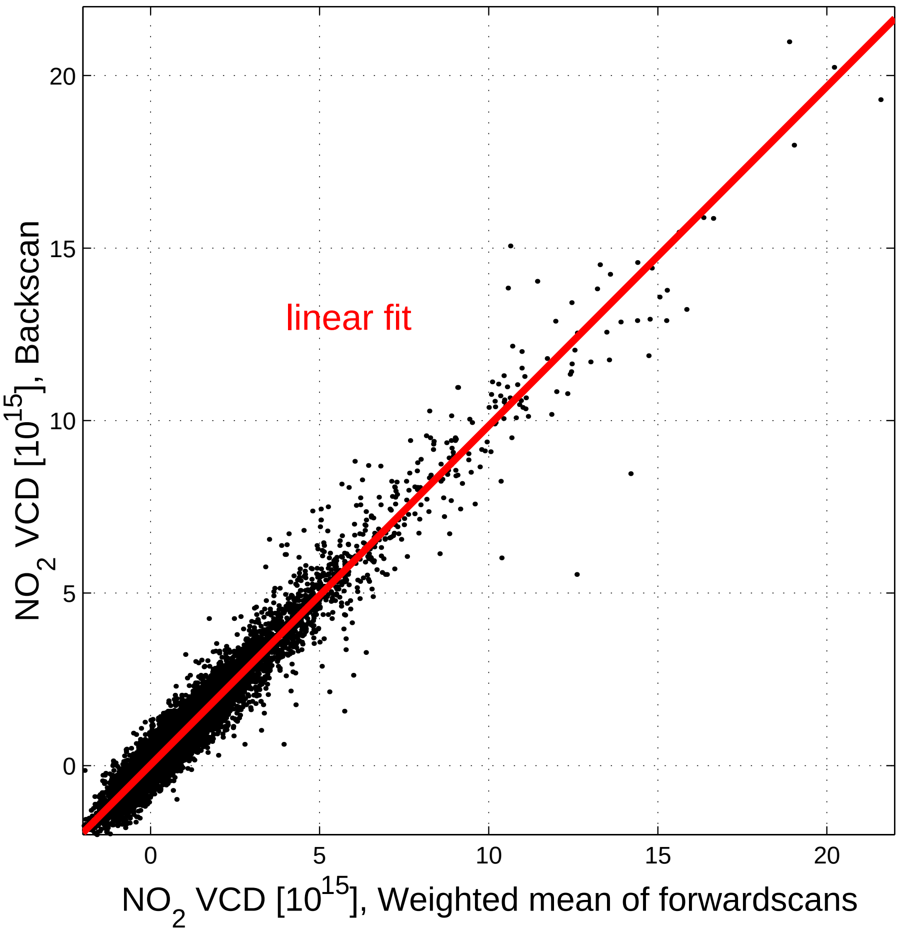

Fig. 9. Correlation of the mean NO_2 VCD of the NSM forwardscans and the respective backscan (all NSM observations over the US, Europe, China and Japan). The slope of the linear fit is 0.98.

ACPD

4, 1665–1689, 2004